

Yu. A. Buevich and M. I. Yakushin

Zhurnal Prikladnoi Mekhaniki i Tekhnicheskoi Fiziki,
Vol. 9, No. 1, pp. 56-65, 1968

The authors examine a most simple model of mass transfer from the heated surface of a condensed phase in the presence of chemical reactions. It is shown that decomposition (or sublimation) of the molecules of starting substance and subsequent vaporization (or sublimation) of the decomposition products have an important influence on this process and lead to the appearance of a number of new effects not observed in the ablation of nondecomposing materials. The principal conclusions of the theory are confirmed qualitatively by the experimental data, on the degradation of certain polymers in a high-enthalpy gas jet described in the concluding section of the paper.

§1. Formulation of the problem. In the general case ablation in a gas flow is described by a system of equations of hydrodynamics, of convective heat transfer, and of diffusion, written separately for the two phases with allowance for that evolution (or absorption) of the heat and mass of all components which is due to the reactions in the system. This problem is strongly nonlinear and difficult to solve even in the simplest cases. Accordingly, in what follows we employ every possible simplifying assumption without distorting the qualitative characteristics of the ablation process.

We consider a plane phase interface $\xi = \xi_0(t)$, assuming that the undecomposed condensed phase consists of type AB molecules and that a single decomposition reaction $AB \rightarrow A + B$ is possible in this phase. Let the activation energy and the absorbed energy per AB molecules be equal to ε and \dot{e} , respectively. We neglect the reverse reaction of synthesis of AB molecules from A and B molecules, assuming that in the temperature interval considered the rate constant of this reaction is much lower than the rate constant of the forward reaction $k^+(T)$.

The processes of heat transfer and removal of the vapors of the substances AB, A, and B in the gas phase depend on the flow conditions at the surface, on the presence of reactions in the gas phase, etc. For our purposes there is no need to be too specific about the nature of these processes; accordingly, we consider them within the framework of the Nernst diffusion-layer theory, neglecting, for simplicity, all reactions in the gas phase, including the reaction $AB \rightarrow A + B$. Thus, we assume that for each transport processes there is a layer of the thickness Δ , adjacent to the ablation surface and such that within the layer transport is effected by a molecular mechanism, while at its outer boundary relaxation to the external conditions is almost instantaneous. The quantities Δ depend on the conditions in the high-enthalpy gas flow and on the intensity of vaporization processes at the surface itself, which determines the Stefan flux and can be formally introduced in terms of the heat- and mass-transfer coefficients [1].

We assume that the molecular transport coefficients do not depend on the temperature and composition of the gas phase, and we use an approximation of independent diffusion, neglecting thermal diffusion and considering the concentrations of the components instead of their partial pressures in the gas phase.

Also neglecting the Knudsen-Langmuir layer and the motion of the ablation surface, we arrive in the region $\xi < \xi_0(t)$ at the problem:

$$\begin{aligned} \frac{\partial T}{\partial t} &= a\Delta T, & \frac{\partial c_i}{\partial t} &= D_i\Delta c_i, & T|_{x=\Delta} &= T_0, \\ c_i|_{x=\Delta} &= 0, & T|_{x=0} &= T_s, & c_i|_{x=0} &= q_i, \\ x &= \xi - \xi_0(t), & i &= 0, 1, 2. \end{aligned} \quad (1.1)$$

Here a and D_i are the thermal diffusivity and diffusion coefficients, the values of subscript $i = 0, 1$, and 2 are assigned to the substances AB, A, and B, respectively, and q_i denotes the instantaneous values their vapor concentrations at the ablating surface. For q_i we write the equations

$$q_i = s_i n_i q_i^0, \quad (1.2)$$

where s_i denotes the small areas occupied by a single molecule of the substances AB, A, or B; n_i denotes the surface concentrations of these substances in the condensed phase; q_i^0 is the saturated vapor concentration over the surface of the pure i -th substance. In (1.2) we have assumed, for simplicity, that the probability of one molecule of a certain substance escaping into the gas phase is proportional to the fraction of the area occupied by this substance on the surface of the condensed phase. This assumption is valid at small concentrations and in this case corresponds to the Henry and Raoult laws. In the general case, of course, it represents a certain idealization of the vaporization process.

In the region $\xi_0(t)$ (or $x < 0$) it is also possible to write transport equations analogous to Eqs. (1.1) with allowance for the decomposition reaction $AB \rightarrow A + B$ in the condensed phase. However, if the activation energy ε is sufficiently large, in accordance with the general method used in combustion theory [1] it can be assumed that the reaction proceeds only in a narrow zone of thickness δ , adjacent to the phase interface. This assumption is confirmed by numerous experiments on the heterogeneous combustion of decomposing propellants and by data on the ablation of a number of polymers in a plasma jet (see [2] and §4 of this paper). In a nonstationary process of thermal decomposition the quantity δ depends generally speaking, on time, while under stationary conditions

$\delta \approx \text{const.}$ However, in any case, δ depends on the surface temperature T_S , but this dependence is much weaker than the dependence on T_S of the rate constant $k'(T)$.

For stationary conditions it is possible to write the mass-balance equations of the components in the form:

$$\begin{aligned} -k(T_s)n_0 + D_0 \frac{dc_0}{dx} \Big|_{x=0} + \gamma &= 0, \\ n_0 = N_0^{1/2} \Big|_{x=0} \quad (\gamma = uN), \quad k(T_s)n_0 + D_j \frac{dc_j}{dx} \Big|_{x=0} &= 0, \\ n_j = N_j^{1/2} \Big|_{x=0} \quad (j=1, 2). \end{aligned} \quad (1.3)$$

The effective value of $k(T_S)$ is given by

$$k(T_S)n_0 \approx \int_{-\delta}^0 k'(T) N_0 dx \quad (1.4)$$

In (1.3) and (1.4) N_0 is the volume concentration of AB molecules, $N_0|x \rightarrow \delta = N$, and u and γ are the linear and molar rates of mass transfer from the surface $x = 0$. In the case of a purely heterogeneous reaction $k(T_S) = k'(T_S)$.

The calorimetric equation has the form:

$$\begin{aligned} Q_0 = \lambda \frac{dT}{dx} \Big|_{x=0} = \\ = ek(T_s)n_0 - \sum_{i=0}^2 r_i D_i \frac{dc_i}{dx} \Big|_{x=0} + Q_r = Q_s. \end{aligned} \quad (1.5)$$

Here λ is the thermal conductivity of the gas phase; r_i is the sum of the internal and external heats of vaporization per molecule of i th substance; $Q_r(T_S)$ denote the radiative heat losses. The quantity $Q_0(T_S)$ represents the total external flow of heat to the ablation surface, while $Q_s(T_S)$ is the amount of heat absorbed per unit area of this surface.

The surface concentrations n_i must satisfy the obvious compatibility condition

$$\begin{aligned} n_0 + \mu_1 n_1 + \mu_2 n_2 = N^{1/2}, \quad \mu_1 + \mu_2 = 1 \\ \mu_i = s_i/s_0 \end{aligned} \quad (1.6)$$

In the case of a material decomposing in a vacuum, instead of (1.3) and (1.5) we have

$$\begin{aligned} -k(T_s)n_0 - g_0(T_s)n_0 + \gamma &= 0, \\ k(T_s)n_0 - g_j(T_s)n_j &= 0, \\ (j=1, 2) \\ Q_0 = Q_s = ek(T_s)n_0 + \sum_{i=0}^2 r_i g_i(T_s)n_i + Q_r(T_s). \end{aligned} \quad (1.7)$$

Here, Q_0 is the energy arriving at a unit area of the interface due to radiative heating. The quantities g_i in (1.7) represent the rate constants for the escape of AB, A, and B molecules from the condensed phase.

From Eqs. (1.3) and (1.6) or the first ones of Eqs. (1.7) and (1.6) we obtain simple expressions for the molar rate of ablation

$$\gamma = - \sum_{i=0}^2 \mu_i D_i \frac{dc_i}{dx} \Big|_{x=0} \quad \text{or} \quad \gamma = \sum_{i=0}^2 \mu_i g_i n_i \quad (1.8)$$

§2. Investigation of stationary regimes. We consider stationary solutions for the problem formulated above.

From (1.1) we obtain

$$\begin{aligned} T = T_0 + (T_s - T_0)(1 - x/\Delta^*), \\ c_i = q_i(1 - x/\Delta_i). \end{aligned} \quad (2.1)$$

Solving the remaining equations, after computations we obtain

$$\begin{aligned} n_j = n_0 f_j, \quad n_0 = \frac{N^{1/2}}{1 + \mu_1 f_1 + \mu_2 f_2}, \\ \gamma = g_0 N^{1/2} \frac{1 + f_0}{1 + \mu_1 f_1 + \mu_2 f_2}, \\ \lambda \frac{T_0 - T_s}{\Delta^*} = r_0 g_0 N^{1/2} \frac{1 + \alpha f_0}{1 + \mu_1 f_1 + \mu_2 f_2} + Q_r(T_s) \\ \alpha = \frac{\varepsilon + r_1 + r_2}{r_0}, \quad g_i = \left(\frac{D}{\Delta} s q^0(T_s) \right)_i, \\ f_i = \frac{k(T_s)}{g_i(T_s)}. \end{aligned} \quad (2.2)$$

Here, the quantities g_i represent the rate constants of the processes of vapor removal, while f_i denote the ratios of the decomposition-reaction rate to the removal rates. We note that the solution of problem (1.6) and (1.7) also leads to expressions (2.2) with the g_i from (1.7).

To be specific, we assume that the dependence of k and g_i on T_S can be represented approximately by the Arrhenius expressions

$$\begin{aligned} k(T) = K \exp\left(-\frac{\varepsilon}{\theta}\right), \quad g_i(T) = G_i \exp\left(-\frac{\varepsilon_i}{\theta}\right), \\ \theta = kT, \quad f_i(T) = F_i \exp\left(-\frac{\varepsilon - \varepsilon_i}{\theta}\right), \quad F_i = \frac{K}{G_i} \end{aligned} \quad (2.3)$$

Here, ε_i denote quantities with the significance of activation energies of processes of escape of AB, A, and B molecules into the gas phase. These quantities can be determined approximately from empirical Antoine relations for saturated vapor concentrations. The symbols K and G_i have the significance of normal frequency factors, and k is the Boltzmann constant.

The decomposition of AB molecules is associated with the disruption of strong intramolecular chemical bonds, and the processes of molecular escape into the gas phase are linked with the disruption of relatively weak intermolecular bonds (van der Waals forces, hydrogen bridges, etc.). Therefore it is possible to assume $\varepsilon < \varepsilon_i$ ($i = 0, 1, 2$). To be specific, we further assume that $\varepsilon_1 > \varepsilon_2$, so that on a certain interval $0 < \theta \leq \theta_0$, we have $\mu_2 f_2 \ll \mu_1 f_1$. It is clear from (2.2) and (2.3) that in this interval the quantity $n_1(\theta)$ increases monotonically, $n_2(\theta) \approx 0$, and $n_0(\theta)$ decreases monotonically. In the region $\theta > \theta_0$, $n_2(\theta)$ begins to increase appreciably, while, depending on the ratio of the quantities $\mu_j f_j$, the surface concentration $n_1(\theta)$ of the less readily vaporizable decomposition product can both increase and decrease with increase in θ . The characteristic curves of $n_i(\theta)$ are presented for the latter case in Fig. 1; as $\theta \rightarrow \infty$ they all tend to a plateau.

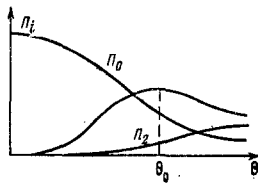


Fig. 1

In particular cases the ablation rate γ will be given by the expressions

$$\begin{aligned} \gamma(\theta) &\approx \gamma_0(\theta) = g_0 N^{1/2} = N^{1/2} G_0 \exp(-\varepsilon_0/\theta) \text{ at } f_i(\theta) \ll 1, \\ \gamma(\theta) &\approx N^{1/2} K \exp(-\varepsilon/\theta) \text{ at } f_j(\theta) \ll 1, f_0(\theta) \gg 1, \\ f_2(\theta) &\ll 1, f_0(\theta) \ll 1, f_1(\theta) \gg 1, \\ \gamma(\theta) &\approx N^{1/2} \frac{G_0 G_1}{\mu_1 k} \exp \frac{\varepsilon - \varepsilon_0 - \varepsilon_1}{\theta}, \\ (i=0, 1, 2; j=1, 2). \end{aligned} \quad (2.4)$$

In the first case (at low temperatures) the decomposition and mass transport are determined by the kinetics of vaporization and removal of the vapors of the starting substance AB, and in the second by the kinetics of the decomposition reaction. In the third case the mass-transfer rate is affected by the processes; in this case the quantity $\gamma(\theta)$ decreases with increase in θ , provided that $\varepsilon_0 + \varepsilon_1$ (the inequality with respect to $f_i(\theta)$ in (2.4) is realized by means of appropriate normal frequency factors in (2.3)). We then have the expansion

$$\begin{aligned} \gamma(\theta + \delta\theta) &\approx \gamma(\theta) (1 + \beta\theta^{-2}\delta\theta), \quad \beta = \varepsilon_0 + \varphi_0 - \varphi_1, \\ \varphi_0 &= \frac{(\varepsilon - \varepsilon_0) f_0}{1 + f_0}, \quad \varphi_1 = \frac{\mu_1(\varepsilon - \varepsilon_1) f_1 + \mu_2(\varepsilon - \varepsilon_2) f_2}{1 + \mu_1 f_1 + \mu_2 f_2}. \end{aligned} \quad (2.5)$$

The quantity β is less than zero if the inequality

$$\begin{aligned} \varepsilon(\mu_1 f_1 - f_0) &> \varepsilon_0(1 + \mu_1 f_1) + \varepsilon_1 \mu_1 f_1 (1 + f_0), \\ 0 < \theta &\leq \theta_0. \end{aligned}$$

is satisfied.

Hence it is clear that the occurrence of an anomalous section on the $\gamma(\theta)$ curve, where the derivative of $\gamma(\theta)$ with respect to θ is negative, is favored by an increase in $\mu_1 f_1$, and a decrease in f_0 , i. e., the decomposition product A is less readily vaporized than the substance AB.

At $\theta \sim \theta_0$ let this inequality not be satisfied, i. e., $\beta > 0$. If as θ falls the quantity f_0 decreases much more rapidly than $\mu_1 f_1$, then β can change sign in a certain interval $\theta_1 \leq \theta \leq \theta_1' < \theta_0$. Thus, the two types of anomalous segments shown in Figs. 2a and b are possible. At $\theta > \theta_0$ the quantity $\mu_2 f_2$ can be

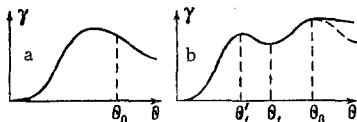


Fig. 2

comparable with $\mu_1 f_1$, and then yet another anomalous segment can appear (see the dashed line in Fig. 2b).

The function $Q_S(\theta)$ behaves similarly. At $\alpha = 1$ and $Q_T(\theta) \approx 0$ (this is possible at not large θ) complete similarity of the relations $\gamma(\theta)$ and $Q_S(\theta)$ is observed. As α increases, the anomalous segments of the function $Q_S(\theta)$ grow shorter, and at $\alpha > 1$ (this is possible if the reaction $AB \rightarrow A + B$ is exothermic they can become broader than the anomalous segments of $\gamma(\theta)$). Clearly, as the number of reactions involved in the process increases, the number of such anomalous segments, generally speaking, increases, and their distribution becomes more peculiar. In the general case, the presence anomalous segments on the curves $\gamma(\theta)$, $Q_S(\theta)$ etc., leads to a nonmonotonic dependence of the ablation rate γ on the amount of heat absorbed at the surface of the ablating material, etc.

Consequently, different stationary temperatures T_S and molar mass-transfer rates can correspond to the same heat flux $Q_0(T_S)$. Conversely, a given mass-transfer rate can be observed under very different heat conditions as the ablating surface. Due allowance for these circumstances is very important in designing heat shields, especially when the specifications require minimization of the total weight without detriment to certain standard shielding properties, as, for example, in the case of aircraft and missile thermal insulation. In principle, there is a possibility of attaining this goal by choosing material on whose surface there is formed a dense layer of a not readily vaporizable substance that partially blocks mass transfer.

§3. Linear stability of stationary regimes in the diffusion region. The stationary regimes of thermal decomposition of a material in a high-enthalpy flow are determined by the points of intersection of the curves $Q_0(T_S)$ and $Q_S(T_S)$ (Fig. 2). Clearly, even in the simplest case, considered in §2, there can be several stationary regimes, so that the question of their stability arises.

In the general case, analysis of stability requires solution of the nonstationary problem of heat- and mass-transfer in both phases. An exception is decomposition in the diffusion region, when the rate of mass transfer is limited by the rate of diffusion transport of the vapors of the components from the surface of the condensed phase, and quasistationary values of the concentrations and n_i and q_i^0 which represent certain functions of the surface temperature T_S (known from the solution of the corresponding stationary problem [1]), are established on that surface itself.

For small perturbations (denoted below by an asterisk) the linearized equations corresponding to the equations (1.1), (1.5), and (1.8) then have the form:

$$\begin{aligned} \frac{\partial T^*}{\partial t} &= a \Delta T^*, \quad \frac{\partial c_i^*}{\partial t} = D_i \Delta c_i^*, \\ \lambda \left(\frac{d^2 T}{dx^2} \Big|_{x=0} \xi^* + \frac{\partial T^*}{\partial x} \Big|_{x=0} \right) &= \\ = - \sum_{i=0}^2 r_i D_i \left(\frac{d^2 c_i}{dx^2} \Big|_{x=0} \xi^* + \frac{\partial c_i^*}{\partial x} \Big|_{x=0} \right) + \end{aligned}$$

$$+ e \left(n_0 \frac{dk}{dT_s} T_s^* + k n_0^* \right) + \frac{dQ_r}{dT_s} T_s^*,$$

$$\gamma^* = - \sum_{i=0}^2 \mu_i D_i \left(\frac{d^2 c_i}{dx^2} \Big|_{x=0} \xi^* + \frac{\partial c_i}{\partial x} \Big|_{x=0} \right),$$

$$n_i^* \approx \frac{dn_i}{dT_s} T_s^*, \quad q_i^{0*} \approx \frac{dq_i^0}{dT_s} T_s^*, \quad i=0, 1, 2. \quad (3.1)$$

Here, ξ^* is a small perturbation of the position of the interface.

The following conditions (we assume for simplicity that $\Delta^* \approx \text{const}$ and $\Delta_i \approx \text{const}$) are imposed on the small perturbations of temperature and concentration:

$$\begin{aligned} T^* |_{x=\Delta^*} = c_i^* |_{x=\Delta_i} = 0, \quad T^* |_{x=0} = T_s^* - \frac{dT}{dx} \Big|_{x=0} \xi^* \\ c_i^* |_{x=0} = s_i (q_i^0 n_0^* + q_i^{0*} n_i) - \frac{dc_i}{dx} \Big|_{x=0} \xi^*, \\ \frac{d\xi^*}{dt} = - \frac{\gamma^*}{N} = -u^*. \end{aligned} \quad (3.2)$$

We represent the perturbations in the form:

$$\{T^*, c_i^*, u^*, \xi^*\} = \{\tau(x), \sigma_i(x), U, \Xi\} e^{\omega t + i x y}.$$

From (3.1), (3.2), and (2.1), we obtain the problem:

$$\begin{aligned} \frac{d^2 \tau}{dx^2} = \left(\kappa^2 + \frac{\omega}{a} \right) \tau, \quad \frac{d^2 \sigma_i}{dx^2} = \left(\kappa^2 + \frac{\omega}{D_i} \right) \sigma_i, \\ \tau |_{x=\Delta^*} = \sigma_i |_{x=\Delta_i} = 0, \quad \tau |_{x=0} = \tau_s - \frac{T_0 - T_s}{\Delta^*} \Xi, \\ \sigma_i |_{x=0} = \frac{d(s_i n_i q_i^0)}{dT_s} \tau_s + \frac{s_i n_i q_i^0}{\Delta_i} \Xi, \\ NU = - \sum_{i=0}^2 \mu_i D_i \frac{d\sigma_i}{dx} \Big|_{x=0}, \quad \Xi = - \frac{U}{\omega}, \\ \lambda \frac{d\tau}{dx} \Big|_{x=0} = \\ = - \sum_{i=0}^2 r_i D_i \frac{d\sigma_i}{dx} \Big|_{x=0} + e \frac{d(kn_0)}{dT_s} \tau_s + \frac{dQ_r}{dT_s} \tau_s. \end{aligned} \quad (3.3)$$

The solution of the first four equations in (3.3) has the form:

$$\begin{aligned} \tau(x) = \left(\tau_s + \frac{T_0 - T_s}{\Delta^*} \frac{U}{\omega} \right) \frac{e^{-lx} - e^{-l(2\Delta^* - x)}}{1 - e^{-2l\Delta^*}}, \\ l = \left(\kappa^2 + \frac{\omega}{a} \right)^{1/2}, \\ \sigma_i(x) = \left(\frac{d(s_i n_i q_i^0)}{dT_s} \tau_s - \frac{sn_i q_i^0}{\Delta_i} \frac{U}{\omega} \right) \frac{e^{-m_i x} - e^{-m_i(2\Delta_i - x)}}{1 - e^{-2m_i \Delta_i}}, \\ m_i = \left(\kappa^2 + \frac{\omega}{D_i} \right)^{1/2}. \end{aligned} \quad (3.4)$$

From the fifth equation in (3.3), and with (3.4), we obtain the expression

$$\begin{aligned} U = \frac{R_1}{R_2} \tau_s, \quad R_1 = 2 \sum_{i=0}^2 \left(\frac{\mu D m}{1 - e^{-2m\Delta}} \frac{d(s_i n_i q_i^0)}{dT_s} \right)_i, \\ R_2 = N + \frac{2}{\omega} \sum_{i=0}^2 \left(\frac{\mu D m}{1 - e^{-2m\Delta}} \frac{sn_i q_i^0}{\Delta} \right)_i. \end{aligned} \quad (3.5)$$

The characteristic equation is obtained from the calorimetric condition after substituting (3.4) and (3.5). It has the form:

$$\omega S_1 R_2 = S_2 R_1, \quad (3.6)$$

where S_j and R_j are certain functions of ω , κ and the parameters of the problem.

In order to simplify, we consider only the situation in which $\Delta^* = \Delta_i = \Delta$, $a = D_i = D$, and $l = m_i = m$. In this case, we have the expressions

$$\begin{aligned} R_1 = \psi(\omega, \kappa) a_1, \quad R_2 = \omega^{-1} \psi(\omega, \kappa) a_2 + N, \\ S_1 = \psi(\omega, \kappa) b_1 + b_0, \quad S_2 = \psi(\omega, \kappa) b_2, \\ a_1 = D \sum_{i=0}^2 \mu_i \frac{d(s_i n_i q_i^0)}{dT_s}, \quad a_2 = \frac{D}{\Delta} \sum_{i=0}^2 (\mu s_i n_i q_i^0)_i, \\ b_0 = e \frac{d(kn_0)}{dT_s} + \frac{dQ_r}{dT_s}, \quad b_1 = \lambda + D \sum_{i=0}^2 r_i \frac{d(s_i n_i q_i^0)}{dT_s}, \\ b_2 = \lambda \frac{T_0 - T_s}{\Delta} - \frac{D}{\Delta} \sum_{i=0}^2 (r_i s_i n_i q_i^0)_i, \\ \psi(\omega, \kappa) = \frac{2m}{1 - e^{-2m\Delta}}. \end{aligned} \quad (3.7)$$

We consider the disturbance of stability at large κ , when it is possible to assume that $|\psi(\omega, \kappa)| \gg |b_0|/|b_1|$. In this case, in the expressions for S_1 in (3.7) the second term is much smaller than the first and Eq. (3.6) has the form:

$$\omega = z(\omega, \kappa) = (N b_1)^{-1} (a_1 b_2 - a_2 b_1) \psi(\omega, \kappa). \quad (3.8)$$

The solutions of this equation, which correspond to instability, can be represented in the form $\omega = \omega_0^2 e^{i\varphi}$, where $|\varphi| < (1/2)\pi$; Eq. (3.8) decomposes in two real equations for the moduli and arguments of the left- and right-hand sides of (3.8). For $\kappa \sim 0$ the second equation has the form:

$$\begin{aligned} \varphi = 1/2 \varphi - \chi, \quad \chi = \\ = \arg \{1 - \exp[-d\omega_0 e^{i\varphi/2}]\}, \quad d = 2D^{-1/2}. \end{aligned}$$

After computations, for χ we obtain the relation

$$\chi = \arctg \frac{e^{-d\omega_0} \sin [d\omega_0 (1 - \xi^2)^{1/2}] \text{sign } \varphi}{1 - e^{-d\omega_0} \cos [d\omega_0 (1 - \xi^2)^{1/2}]}$$

Here, $\xi = \cos(\varphi/2)$ varies in the interval $(2^{-1/2}, 1]$. It is easy to see that the sign of χ coincides with the sign of φ , and $|\chi| < (1/2)|\varphi|$; a similar situation also exists, to an even greater degree, in the general case $\kappa \neq 0$, so that Eq. (3.8) cannot be satisfied if $R\omega > 0$ and $\varphi \neq 0$. Hence it follows that increasing perturbations correspond to real ω . As can easily be seen from (3.8), the regions of instability are defined by the inequality

$$b_1^{-1} (a_1 b_2 - a_2 b_1) > 0 \quad (3.9)$$

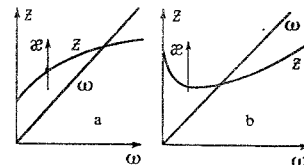


Fig. 3

Stability is immediately disturbed with respect to small perturbations of all wavelengths, and at a low level of supercriticality ω increases monotonically with increase in the wave number κ (Fig. 3a, which shows the ω and z curves from (3.8) when condition (3.9) is satisfied).

In the opposite limiting case of small κ , so that $S_1 \approx b_0$, it is also easy to show that the growing perturbations have zero frequency. In this case the regions of instability are defined by the inequalities

$$b_0^{-1} (a_1 b_2 \psi(0, \kappa) - a_2 b_0) > 0. \quad (3.10)$$

and the characteristic equation is similar in form to (3.8), but

$$z(\omega, \kappa) = (N b_0)^{-1} (a_1 b_2 \psi(\omega, \kappa) - a_2 b_0) \psi(\omega, \kappa).$$

The ω and z curves are shown qualitatively in Fig. 3b. It follows from (3.10) that under certain conditions instability is possible with respect to perturbations not accompanied by a change in the shape of the ablating surface.

With expressions (3.7) it is easy to determine the regions of instability (3.9) and (3.10) in terms of various physical quantities relating to the stationary state, namely, the ablation rate γ , the heat fluxes Q_0, Q_S, Q' , and Q'' (here, Q' is the absorption of heat due to the reaction and to surface radiation; Q'' is the absorption of heat as a result of vaporization), and their derivatives with respect to T_S . Physically, such an analysis leads to the following instability condition: the stationary ablation regime is unstable with respect to small perturbations if the temperature variation of parts of the surface which are convex in the direction of the gas phase is positive, and the stationary ablation rate is anomalous, or if the above-mentioned variation is negative, and $\gamma(T_S)$ increases with increase in T_S . The causes of instability of this type are similar in many respects to the causes of the diffusional-thermal instability of the plane front of a laminar flame [3]. In both cases the velocity of the parts of the perturbed surface which are convex in the direction of its motion increases, while the velocity of concave parts decreases in comparison with the stationary velocity as a result of changes in the thermal and diffusional conditions close to the surface. If all possible stationary regimes are unstable, obviously, a self-oscillating ablation regime is established.

We note that the regions of instability depend differently on the heat fluxes Q' and Q'' and on their derivatives with respect to T_S . They are essentially different for cases of exothermic and endothermic decomposition surface. At very large κ the results derived above cease to be valid, since the decomposition surface is no longer equally accessible, and the above assumptions relating to the quantities Δ and to quasistationarity can be inadequate [1].

We note that instability of the same type should also be observed in connection with thermal decomposition processes complicated by other reactions between the parent substance or its decomposition products and various components of the gas phase, for example, combustion. Instability of a conical propellant surface

was observed experimentally, for example, in [4]. Instability of the type in question is evidently the chief reason for the appearance of ripples on propellant surface under erosive burning conditions.

§ 4. Experimental. The authors conducted experiments on the thermal decomposition of specimens of certain polymer materials in a low-temperature plasma jet. A number of materials (polypropylene polystyrene) are characterized by a typically bulk mechanism of pyrolysis with the evolution of gaseous products over almost the entire thickness of the specimen, but polyethylene and teflon are observed to have a surface mechanism of decomposition that, generally speaking, fits within the framework of the assumption made above. We will briefly describe certain results of tests on the last two materials, pertinent to the subject of this paper.

The experiment were conducted on an apparatus in which a high-frequency electrodeless discharge was used to heat the gas jet (argon or air at 1 atm). As a result a steady plasma jet was created close to the inductor; the flow velocity was of the order of 100 m/sec; the diameter of the working section of the jet was about 40 mm; temperature of the latter reached 900° K and varied by not more than 100–150° K in the radial direction. Detailed measurements were made of the energy supplied to the plasma, of the heat fluxes in various sections of the jet, etc.

The cylindrical specimens of polyethylene and teflon were 6 and 11 mm in diameter; they were mounted on a special water-cooled holder and were introduced almost instantaneously in the working section of the jet, coaxially with the latter. The heat flow to the forward end face of the specimens in the argon plasma amounted to 0.4 to 0.5 kW/cm², and in the air plasma up to 1 kW/cm². During decomposition process the specimens were filmed on special color and infrared films, sensitized in narrow spectral intervals. By analyzing the films it was possible to estimate the integral and local rates of mass transfer, the structure of the boundary layer, etc., and to register the brightness temperature of the surface along the length of the specimen at different times after the beginning of the experiment. This was done by measuring the blackening of the frames on a microphotometer; as a standard we used the incandescent anode spot of a carbon arc.

The principal results of the experiments can be summarized as follows.

1. On the surface of the decomposing material there is formed a layer in which the concentration of one of the decomposition products—carbon (carbonaceous residue—is sharply increased. At approximately identical heat fluxes the thickness of this layer was much smaller in an air plasma than in an argon plasma. This is due to the removal of carbon as a result of its heterogeneous combustion in an oxidizing atmosphere. This effect is clearly visible in photographs of polyethylene specimens exposed to argon and air plasma (Figs. 4a, b, respectively). At small heat fluxes a carbonaceous layer is not generally formed; as the flux increases, its thickness gradually grows, reaches a maximum, and then begins to fall. For example, Fig. 5 presents photographs of teflon specimens tested in an air plasma. Near the nose of the specimens, where the heat flux is maximum and near the tail, where it is minimum the carbonaceous layer is much more weakly expressed than



Figs. 4a, b

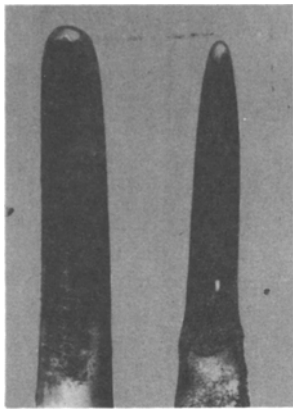


Fig. 5

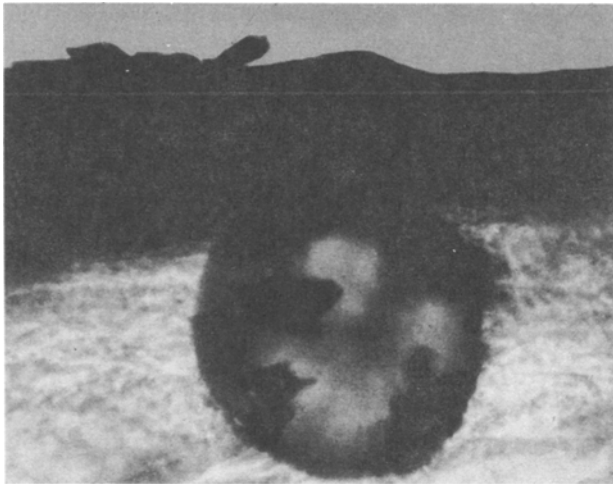


Fig. 6

in the middle, where the heat flux takes certain intermediate values. A decrease in the thickness of the layer with increase in heat flux is also observable in Fig. 4.

2. Thin sections were prepared from various specimens and were used to investigate the thickness and structure of the carbonaceous layer. The thin section of a polyethylene specimen after exposure to an air plasma is shown in Fig. 6 (magnification 500X). There is a fairly distinct boundary between the carbonaceous layer and the undecomposed material. In the same photograph it is also possible to observe a bubble containing gaseous products of pyrolysis and a carbon deposit on the walls which is adjacent to the layer from within. The diameter of this bubble is 26μ . The experiments indicate that in polyethylene such bubbles are very rare, and that the carbon which they carry to the surface forms only a small fraction of the total carbon in the layer. When teflon decomposed, the carbonaceous layer was much thinner, and, in general, internal bubbles evidently did not form.

3. The decomposition of polyethylene specimens proceeds both as a result of vaporization and combustion at the surface and as a result of mechanical ejection of small lumps of materials into the boundary layer. This effect can be followed clearly in motion-picture frames of the decomposing specimen; local defects of the carbonaceous layer are also noticeable in Fig. 4. It can be assumed that the mechanical removal of part of the surface of the specimen is associated with cracking due to thermal stresses and to increase pressure of the gaseous products of pyrolysis beneath the carbonaceous layer. The latter mechanism is especially important in the initial instants, when this layer is still very thin and the material beneath it has not yet

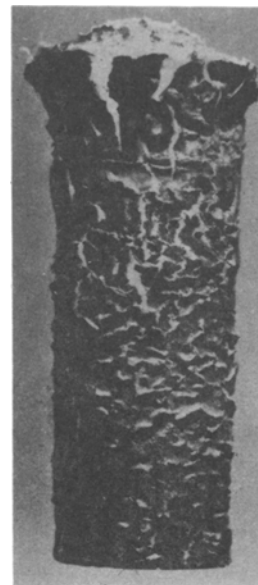


Fig. 7

softened. In this case buckling and local destruction of the carbonaceous layer are observed (Fig. 7).

4. The surface of the specimens displays a ripple, whose amplitude reaches 1 mm or more (for polyethylene). This indicates instability of the decomposition process (Fig. 4 and 7). Two explanations are possible, the first being associated with instability of the type considered above, and the second with the development of wind waves in the softened surface film. The role of these waves has been noted on a number of occasions in publications concerned with the ablation of nondecomposing substances (see, for example, [5]). In our case, in view of the high viscosity of the molten material and of the presence of an overlying rigid carbonaceous film, the second explanation is improbable. A very shallow ripple, apparently of this origin, was observed only at the end face of polyethylene specimens, where the carbonaceous layer is quite thin and where the heat and momentum fluxes to the surface are maximum. Moreover, a shallow regular ripple is also observed on the surface of teflon specimens under conditions when a viscous film is generally absent.

5. Investigations of the brightness temperature of decomposing specimens showed that the surface temperature depends nonmonotonically on the heat flow to the surface. The logarithm of the film density, which is proportional to the brightness temperature (in relative units), is shown in Fig. 8 as a function of the coordinate, reckoned along the axis of the specimen, 1.5, 2.5, 3.5, and 4.5 sec after the beginning of an experiment on teflon. In this figure the sharp position of the tail end of the specimen has been fixed. The sharp

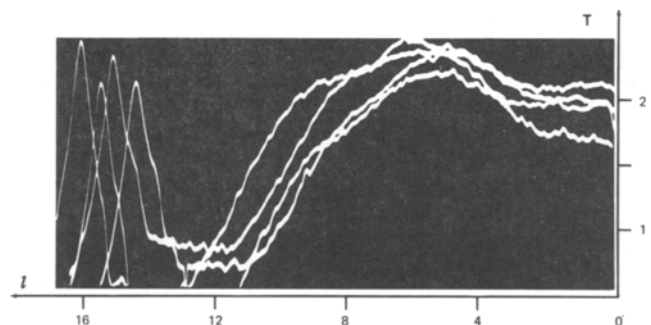


Fig. 8

peak corresponds to the temperature of the boundary layer at the nose of the specimen: at the end face itself the temperature is much lower, but it increases with distance from that face, reaches a maximum, and then decrease. Similar relations are also characteristic of polyethylene specimens. It is likewise evident from Fig. 8 that there are temperature oscillations in the boundary layer and on various section.

of the surface. Periodic changes in luminosity were also observed visually. This apparently corresponds to a self-oscillating decomposition regime, but unfortunately the available experimental material is insufficient to support a definitive conclusion regarding the presence of self-oscillations.

Thus, there is good qualitative agreement between the theoretical conclusions of § 2 and § 3 and the experimental data. Of course, it is too early to talk of a quantitative correspondence, not only on account of the very approximate nature of the model considered but also owing to the extreme complexity and multistage nature of the chemical reactions involved in the process of thermal decomposition of polymer materials.

The authors thank G. I. Barenblatt for his interest in their work.

REFERENCES

1. D. A. Fran-Kamenetskii, Diffusion and Heat Transfer in Chemical Kinetics [in Russian], Izd. Nauka, 1967.
2. C. Huggett, "Combustion of solid propellants," collection: Combustion Processes [Russian translation], Fizmatgiz, p. 430, 1961.
3. G. I. Barenblatt, Ya. B. Zel'dovich, and A. G. Istratov, "The diffusional-thermal stability of a laminar flame," PMTF, 4, 1962.
4. M. E. Wilkins and M. E. Tauber, "Boundary-layer transition on ablating cones at speeds up to 7 km / sec," AIAA J. vol. 4, no. 8, 1966.
5. J. Alhara, "Surface distortion of the molten layer in the axisymmetric stagnation region," AIAA, J. vol. 4, no. 4, 1966.

20 October 1967

Moscow